Author(s): Haarahiltunen, Antti & Varpula, Aapo & Savin, Hele

Title: Modeling the effect of mobile ion contamination on the stability of a microelectromechanical resonator

Year: 2011

Version: Final published version

Please cite the original version:

Haarahiltunen, Antti & Varpula, Aapo & Savin, Hele. 2011. Modeling the effect of mobile ion contamination on the stability of a microelectromechanical resonator. Journal of Applied Physics. P. 5. 0021-8979 (printed). DOI: 10.1063/1.3622511.

AIP Journal of Applied Physics

Modeling the effect of mobile ion contamination on the stability of a microelectromechanical resonator

A. Haarahiltunen, A. Varpula, and H. Savin

Citation: Journal of Applied Physics **110**, 043505 (2011); doi: 10.1063/1.3622511
View online: http://dx.doi.org/10.1063/1.3622511
View Table of Contents: http://scitation.aip.org/content/aip/journal/jap/110/4?ver=pdfcov
Published by the AIP Publishing

Modeling the effect of mobile ion contamination on the stability of a microelectromechanical resonator

A. Haarahiltunen,[a] A. Varpula, and H. Savin
Department of Micro and Nanosciences, Aalto University, PO Box 13500, FI-00076 Aalto, Finland

(Received 29 March 2011; accepted 11 July 2011; published online 17 August 2011)

We present a theoretical model for mobile ion contamination in a silicon microelectromechanical resonator. In the model both drift and diffusion of the mobile charge in dielectric films are taken into account. The model is verified through a comparison to existing experimental data. We show that the model can describe the frequency drift of resonators in a wide temperature range. © *2011 American Institute of Physics*. [doi:10.1063/1.3622511]

INTRODUCTION

Dielectric charging in a radio-frequency microelectromechanical (RF-MEM) switch is widely studied and identified as being one of the major stability problems.[1–3] However, in these studies the electric fields are typically rather high and, therefore, the stability problems are mostly due to the tunneling and trapping of charge carriers in the dielectric film. It is well known that the MEMS processes are vulnerable to mobile ionic contamination, such as sodium and potassium, from wet etching processes. Additional contamination can occur during anodic bonding[4] which is often used for sealing the devices. The effect of the mobile ionic contamination on the stability of microelectromechanical (MEM) devices is much less studied. However, recent experiments by Bahl *et al*. demonstrate that a mobile charge can cause a resonant-frequency drift in an oxidized silicon resonator under a relatively low electric field.[5] The resonant-frequency drift is one of the major barriers to the commercialization of silicon MEM resonators for timing applications.[6,7] Since the contamination is almost inevitable at present, it seems reasonable to also assume that mobile charge contamination can be a significant source of drift in other capacitive MEM components, such as voltage references[8] and accelerometers, which normally operate at lower electric fields than RF-MEM switches.

In this paper we analyze the effect of mobile ionic contamination on long term stability in a capacitive MEM component with oxide layers. We compare theoretical results to the experimental results of Bahl *et al*.[5] in the case of an oxidized silicon MEM resonator.

THEORY

Figure 1 shows the structure that is employed in the analysis of the mobile charge on a moving plate capacitor system. Applying voltage on the capacitor introduces an attractive electrostatic force between the capacitor plates. In the case of a small displacement, Δg, the restoring mechanical force can be described by a single spring constant, $F_m = -k_m \Delta g$ (see Fig. 1). In the steady state, the electrostatic force is balanced by the mechanical force.

The charge distribution in the SiO_2 layers affects the built-in voltage of the device which, in a variable MEM capacitor, can be detected as an electrostatic force offset at a zero DC-bias voltage. This electrostatic force offset corresponds to a shift of minimum from zero in the capacitance–voltage curve. In Refs. 1 and 5 it was shown that the built-in voltage, V_{bi}, can be calculated for the known concentration profile using the formula,

$$V_{bi} = \frac{q}{e_{ox}} \int_0^{t_{ox}} x N_{mob}(x) dx + \frac{q}{e_{ox}} \int_{g+t_{ox}}^{g+2t_{ox}} [x - (g + 2t_{ox})] N_{mob}(x) dx, \quad (1)$$

where N_{mob} is the concentration of the mobile charge, t_{ox} is the thickness of the silicon dioxide, g is the thickness of the air gap, e_{ox} is the permittivity of the silicon dioxide, and q is the elementary charge. Due to the symmetry of the silicon beams, we can assume that there is no Fermi-level difference. Additionally, the doping of silicon is so high that the change in the band bending can be neglected in the employed voltage range. The Fermi-level difference would only add a constant to Eq. (1). However, if the silicon doping is low, the situation is more complicated. The dependence of the built-in voltage on the applied voltage is not only affected by the profile of mobile ion concentration, as is assumed in Eq. (1), but also the change in band bending should be taken into account. Fortunately, we can often ignore the low-doping effect and assume metallic behavior of the silicon electrodes, since high doping is favored in order to avoid high series resistances.

The resonance frequency is determined by the effective spring constant and the effective mass of the resonator. In the linear approximation the electrostatic force is proportional to the small displacement around the steady-state position. At constant DC-bias this can be characterized by the electrical spring constant, $F_e = k_e \Delta g$. Due to the electrical spring constant, the effective spring constant of the resonator is smaller than the mechanical spring constant. This is known as spring softening, which affects the resonance frequency. Consequently, the built-in voltage and resonant frequency, f', have a relationship,[5]

[a]Author to whom correspondence should be addressed. Electronic mail: antti.haarahiltunen@aalto.fi.

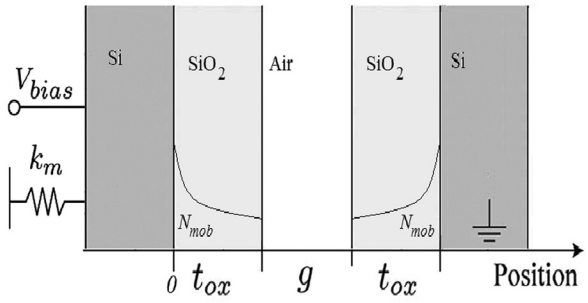

FIG. 1. Illustration of the structure utilized in the analysis of the mobile charge effect. The moving plate is on the left and the stationary plate on the right, respectively. The mobile ion concentration profiles (N_{mob}) are sketched in the equilibrium at zero voltage bias. The mechanical spring constant of the moving plate is k_m.

$$f' \approx f_0\left(1-\frac{k_e}{2k_m}\right)=f_0\left[1-\beta(V_{bias}+V_{bi})^2\right], \qquad (2)$$

where f_0 is the mechanical resonance frequency of the structure, β is a constant, which depends on the mechanical properties of silicon and the geometrical design of the resonator, and V_{bias} is the DC-bias voltage. In these resonators the built-in voltage can be determined from the DC-bias dependence of the resonant frequency.[5,9]

The flux of mobile ions, j, can be calculated using the drift-diffusion theory and the time dependence of the mobile ion concentration, which is given by the continuity equations,

$$j=-qD\frac{\partial N_{mob}(x)}{\partial x}+q\mu N_{mob}(x)E(x), \qquad (3)$$

$$\frac{\partial N_{mob}}{\partial t}=-\frac{\partial}{\partial x}j=D\frac{\partial^2 N_{mob}(x)}{\partial x^2}-\mu\frac{\partial}{\partial x}[E(x)N_{mob}(x)], \qquad (4)$$

where E is the electric field strength, D and μ are the diffusion constant and the mobility of mobile ions, respectively. The electric field is solved using the Poisson equation,

$$\frac{\partial E}{\partial x}=\frac{qN_{mob}}{e_{ox}}. \qquad (5)$$

The boundary condition of Eq. (5) is the total voltage difference across the structure,

$$V_{bias}=\int_0^{g+2t_{ox}} E(x)dx. \qquad (6)$$

The time dependence of the mobile ion concentration is solved from Eqs. (3)–(6) using the no-flux boundary condition at the edges of oxides and the Einstein relation, $D/\mu=kT/q$. Finally, the resonant frequency is calculated using Eq. (2).

RESULTS AND DISCUSSION

Bahl *et al.* studied single-anchored double-ended tuning fork (DETF) resonators fabricated on silicon-on-insulator wafers.[5] Their device is sketched in Fig. 2(a). The thickness of the device layer was 20 μm, the beam length was around

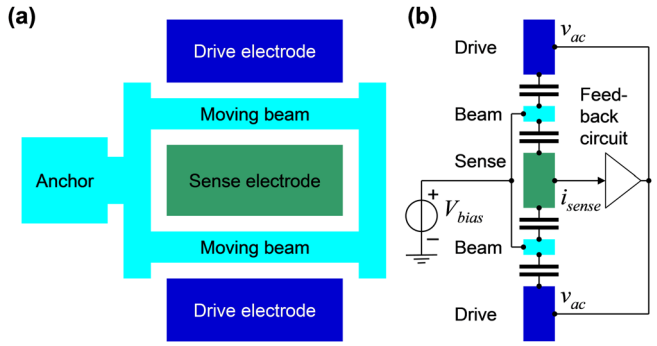

FIG. 2. (Color online) A schematic picture of a single-anchored double-ended tuning fork (DETF) resonator:[5] (a) the layout, and (b) the electrical equivalent circuit in the closed loop measurement scheme.

200 μm, and the lithographically determined actuation gap was 1.5 μm. The resonators were encapsulated using "epi-seal" technology[10] and the silicon surfaces of the resonators were covered with a 350–420 nm thick silicon dioxide layer. In the measurement the actuation was carried out from symmetrically placed drive electrodes on the sides of the two beams. The central electrode was used for sensing the motion of the resonator through capacitive coupling. The structure presented in Fig. 1 can be used in the analysis of the experimental results of Bahl *et al.* since the real device contains four identical capacitors in the DC case, as shown in Fig. 2(b).[5]

In Fig. 3 we present a comparison between the simulated and measured behavior of the resonance frequency during alternating DC-bias voltage stress between 16 and 20 V. The simulated and measured resonant frequencies are in excellent agreement. This suggests that the observed resonant-frequency drift is caused by the movement of the mobile charge only in the structure. After the change in the magnitude of the DC-bias voltage the direction of the frequency drift changes even though the direction of the electric field does not change. From this observation, Bahl *et al.* deduced that there must be some driving force other than the electric field.[5] Naturally, our explanation for the other driving force is the diffusion of mobile ions. At equilibrium at constant temperature, where the net-ion flux is zero ($j=0$ at all x), the concentration profile of the mobile charge only depends on the applied DC-bias voltage. The observed periodical drift in the resonant frequency in Fig. 3 is caused by the mobile ions relaxing to the different equilibrium distributions at 16 and 20 V DC-bias voltages. The equilibrium distributions of the mobile charges after applying 16 V (dashed line) or 20 V (dotted line) DC-bias voltages are shown in Fig. 4.

In the simulations (Figs. 3 and 4) the fitted parameter values, $f_0=1.0617$ MHz, $\beta=4.0540\times10^{-6}$ 1/V^2 and $\mu=4.78\times10^{-13}$ cm^2/Vs, and the parameter values based on the device fabrication steps, $g=1100$ nm and $t_{ox}=420$ nm,[5,11] were used. For the total mobile ionic surface concentration [i.e., $\int_o^{t_{ox}} N_{mob}(x)dx$], we obtained the value of 3×10^{11} cm^{-2} in both oxides. The contamination level of the mobile charge seems to be in a realistic range since the contamination most likely originates from reactive ion etching after unsuccessful cleaning.[5] The fitted mobility value is a factor of 60 lower than the mobility of sodium ions in silicon dioxide, which was extrapolated from the equation,

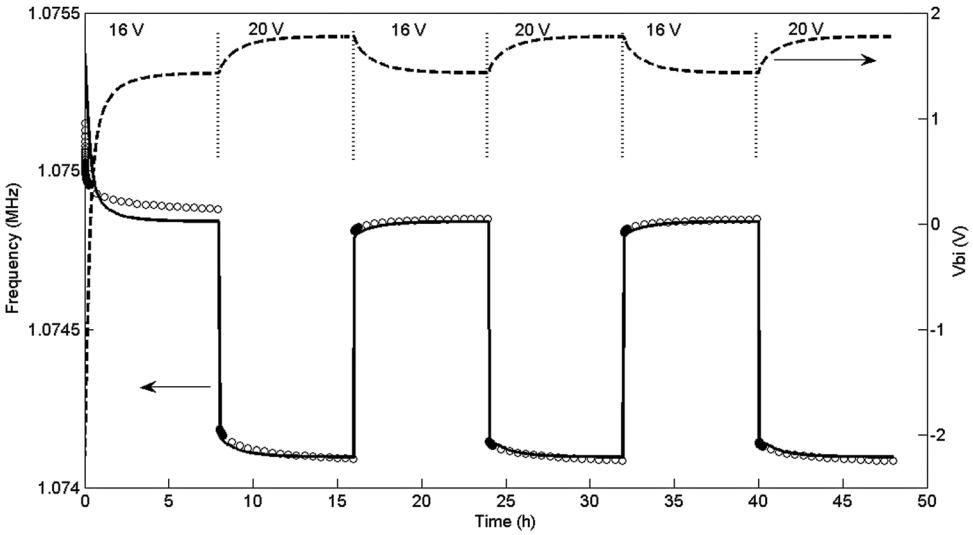

FIG. 3. The simulated behavior of the built-in voltage, V_{bi} (dashed line), and the corresponding resonance frequency (solid line) calculated using Eq. (2), when the bias voltage is alternated between 16 and 20 V at 40 °C. The open circles are the experimentally measured behavior of the resonance frequency from Ref. 5.

3.5×10^{-4} exp(− 0.44 eV/kT), given in Ref. 12. However, when taking into account the variation in the reported values,[13–15] we can conclude that the mobility value is in the typical range for a high mobility contaminant (the most common one being sodium).

The change in the built-in voltage when switching between 16 and 20 V is a few hundred mV (Fig. 3). We simulated the initial condition of the experiment (Fig. 3) as follows: First, the equilibrium condition at zero DC-bias voltage at 40 °C was simulated, which was followed by 2 h at −30 V DC-bias, as in the real experiment. Overall, the initial change of the built-in voltage from −2 to around 2 V and the corresponding change in the resonant frequency (Fig. 2) seem to be overestimated. However, a large shift in the resonant frequency due to negative bias is observed in the beginning of both the simulation and experiment, however some discrepancy remains, although the initial conditions were reproduced as well as possible. One explanation for the difference between the simulations and experiment could be that in the experimental resonator the situation was not completely symmetric as assumed in the simulations. The built-in voltage was detected in the resonators after processing,[5] and can originate from the asymmetric concentration of mobile charges in oxides or asymmetric oxide thicknesses (see Fig. 1). We found that only a slightly better agreement in the simulation of the first 8 h can be achieved when asymmetric concentrations of charges were used. The influence of the DC-bias polarity on the drift was not reported.[5] In this kind of experiment, for example, the initial 30 V bias followed by −16 and −20 V DC-biases, the asymmetric charge concentrations would significantly change the magnitude of the drift.

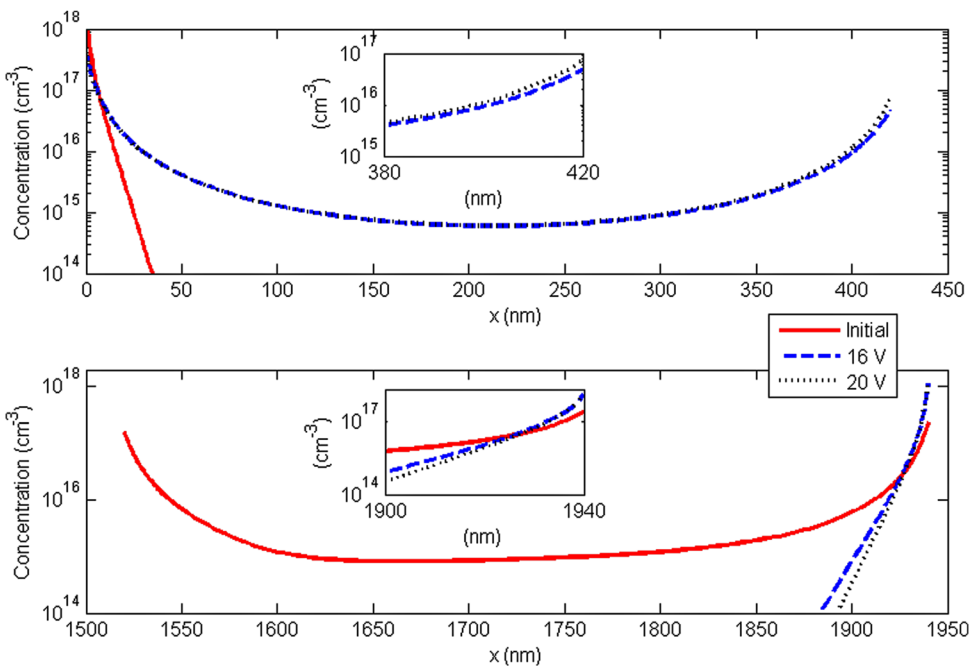

FIG. 4. (Color online) The charge distributions of mobile ions: at the beginning of the experiment (red solid line), at 16 V equilibrium (dashed blue line), and at 20 V equilibrium (dotted black line) DC-bias voltages at 40 °C.

It is known that a fast alternating DC-biasing scheme results in a smaller drift in frequency[16] or in reference voltage,[8] as compared to a constant DC bias. This can be explained by mobile ions having such low mobility that they cannot follow the alternating bias quickly enough. It has also been shown that a MEM-voltage reference is first-order stable against the small change in the built-in voltage, when the total DC-bias voltage is zero. This occurs when the external DC-bias voltage is equal to $-V_{bi}$ [here V_{bi} is as defined in Eqs. (1) and (2)].[8] However, when we consider the mobile ion contamination, this is not necessarily a valid approach, since the drift minimum should occur at the DC-bias voltage, which minimizes the movement of the mobile charge. However, the observation[17] of a drift minimum at a voltage different than $-V_{bi}$ in the structure containing a 50 nm oxide layer suggests that the drift might be due to low-mobility ionic contamination, meaning that a second-order effect dominates the drift. Therefore, the small but persistent drift in oxide resonators in an alternating biasing scheme[16] might indicate that zero DC-bias does not minimize the drift after all. However, Bahl *et al.*[16] suspected an external reason for the drift.

The temperature dependence of the resonant-frequency drift is shown in Fig. 5. The simulated and measured resonant-frequency drifts are again in good agreement. The mobility value of $\mu = 8.75 \times 10^{-6}\ \exp(-0.44\ \text{eV/kT})$ was used in the simulations. The mobility used is a factor of 40 lower than the value predicted by the formula for sodium.[12] The variation of the values of the fitted parameters, f_0 and β, is most probably caused by the temperature dependence of the mechanical properties of the resonator. Unlike the commonly used model[5,9] which utilizes a second-order or a stretched exponential decay function, the drift diffusion model employed here is able to describe the time dependence of the resonant frequency relatively well without the need for any unknown charging processes.

The modeling can easily be used for studying the effect of the mobile ion contamination level of a designed resonator structure. We show an example of this kind of study in Fig. 6, in which we have calculated the maximum drift of the resonance frequency as a function of the contamination level in oxides. The maximum drift is calculated from the difference in built-in potentials at zero volts and 5, 10, or 17 V equilibrium using Eq. (2) with $\beta = 3 \times 10^{-6}\ 1/\text{V}^2$. Figure 5 clearly shows that the drift critically depends upon the contamination level, and that fabrication of a low drift rate oxidized resonator basically requires tight contamination control down to a level ($< 5 \times 10^9\ \text{cm}^{-2}$), which is typical in integrated circuit manufacturing. The maximum drift saturates when the surface contamination is increased; in the presented case saturation occurs around $10^{11}\ \text{cm}^{-2}$. This saturation makes it more difficult to conclude the exact contamination level from the measured drift behavior. At a given contamination level the maximum drift scales down when the thickness of the oxide is reduced, the gap is increased, or the bias voltage is decreased. Of course, all of these parameters are mostly determined by the specifications of the resonator. The contamination effect is merely an nonideality, which can now be separately analyzed.

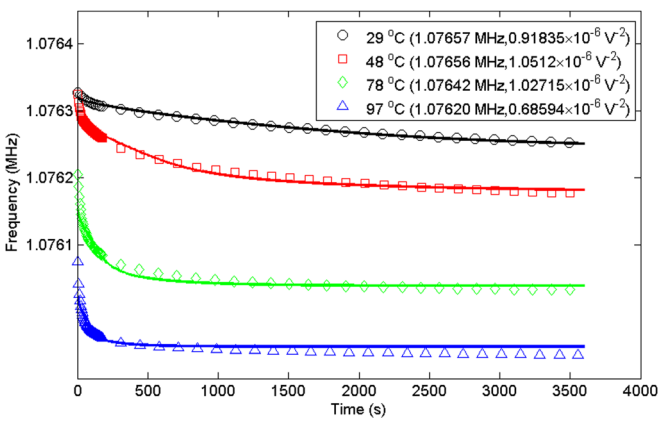

FIG. 5. (Color online) A comparison of the modeled (lines) and measured drift (symbols) of the resonance frequency at temperatures of 29, 48, 78, and 97 °C. The measured data are from Ref. 5. The fitted values of the parameters, f_0 and $\hat{a}$, are shown.

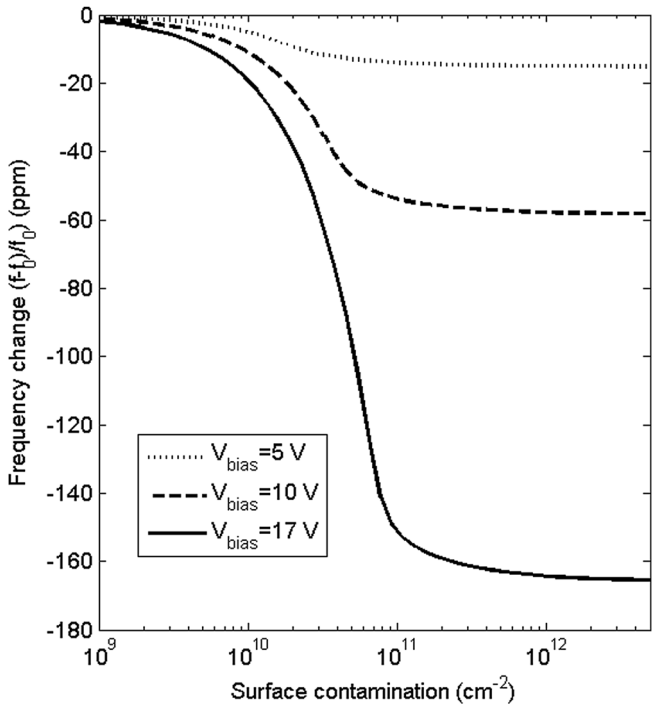

FIG. 6. The calculated maximum resonant frequency drift of the studied resonator structure as a function of the contamination level in the oxides. The applied DC-bias voltages are 5 V (dotted line), 10 V (dashed line), or 17 V (solid line).

In Fig. 6 the time scale of the drift is not indicated. In the case of thin oxides and contaminants with high mobility the drift might already be complete before the actual operation of the device is initiated (i.e., the so-called burn in drift). This kind of drift has less impact on the usage of the device. The opposite is true for thick oxides and contaminants with low mobility.

CONCLUSIONS

We have shown that the theoretical effect of mobile ion contamination on the stability of a silicon resonator is in very close agreement with the experimental observations. The

mobile-ion contamination model gives a simple physical explanation for the beneficial effects of both alternating biasing and additional constant DC-bias voltage schemes for stable MEM device operation. In addition, the model allows for the prediction of drift, when the structure of the resonator and the contamination level is known. This is a great advantage in estimating the large scale manufacturability of devices.

ACKNOWLEDGMENTS

The authors are grateful to Dr. Gaurav Bahl, University of Michigan, Ann Arbor, and to the Stanford Micro Structures and Sensors Laboratory, Stanford University, for providing the details of the experiments and the experimental data. The authors acknowledge the financial support from the Academy of Finland and VTI Technologies Oy.

[1]W. van Spengen, R. Puers, R. Mertens, and I. De Wolf, J. Micromech. Microeng. **14**, 514 (2004).
[2]J. Wibbeler, G. Pfeifer, and M. Hietschold, Sens. Actuators, A **71**, 74 (1998).
[3]D. Molinero and L. Castañer, Appl. Phys. Lett. **94**, 043503 (2009).
[4]K. Schjølberg-Henriksen, G. U. Jensen, A. Hanneborg, and H. Jakobsen, J. Micromech. Microeng. **13**, 845 (2003).
[5]G. Bahl, R. Melamud, B. Kim, S. A. Chandorkar, J. C. Salvia, M. A. Hopcroft, D. Elata, R. G. Hennessy, R. N. Candler, R. T. Howe, and T. W. Kenny, J. Microelectromech. Syst. **19**, 162 (2010).
[6]M. Lutz, A. Partridge, P. Gupta, N. Buchan, E. Klaassen, J. McDonald, and K. Petersen, *Proceedings of the 14th IEEE International Conference on Solid-State Sensors, Actuators and Microsystems*, Lyon, France, June 10–14, 2007.
[7]B. Kim, R. Melamud, R. A. Candler, M. A Hopcroft, C. M. Jha, S. Chandorkar, and T. W. Kenny, *Proceedings of the 2010 IEEE International Frequency Control Symposium*, Newport Beach, USA, June 2–4, 2010.
[8]A. Kärkkäinen, N. Tisnek, A. Manninen, N. Pesonen, A. Oja, and H. Seppä, Sens. Actuators, A **137**, 169 (2007).
[9]S. Kalicinski, M. Wevers, and I. De Wolf, Microelectron. Reliab. **48**, 1221 (2008).
[10]R. Candler, M. Hopcroft, B. Kim, W. Park, R. Melamud, M. Agarwal, G. Yama, A. Partridge, M. Lutz, and T. Kenny, J. Microelectromech. Syst. **15**, 1446 (2006).
[11]R. Melamud, S. A. Chandorkar, B. Kim, H. K. Lee, J. C. Salvia, G. Bahl, M. A. Hopcroft, and T. W. Kenny, J. Microelectromech. Syst. **18**, 1409 (2009).
[12]G. Greeuw and J. F. Verwey, J. Appl. Phys. **56**, 2218 (1984).
[13]J. P. Stagg, Appl. Phys. Lett. **31**, 532 (1977).
[14]R. J. Kriegler and T. F. Devenyi, Thin Solid Films **36**, 435 (1976).
[15]S. R. Hofstein, Appl. Phys. Lett. **10**, 291 (1967).
[16]G. Bahl, J. Salvia, R. Melamud, B. Kim, R. T. Howe, and T. W. Kenny, J. Microelectromech. Syst. **20**, 355 (2011).
[17]A. Kärkkäinen, "A MEMS based voltage references," Doctoral dissertation (Espoo, VTT Publications, 2006).